Journal of Alloys and Compounds 509 (2011) 8783–8787

Contents lists available at ScienceDirect

Journal of Alloys and Compounds

journal homepage: www.elsevier.com/locate/jallcom

As-deformed filament's density and transport currents of MgB_2/Ti/Glidcop wire

P. Kováč[a,*], I. Hušek[a], W. Pachla[b], M. Kulczyk[b], T. Melišek[a], T. Dvorák[c]

[a] Institute of Electrical Engineering, Slovak Academy of Sciences, Dúbravska cesta 9, 841 04 Bratislava, Slovakia
[b] Institute of High Pressure Physics, Polish Academy of Sciences, Sokolowska 29/37, 01-142 Warszawa, Poland
[c] Institute of Materials and Machine Mechanics, Slovak Academy of Sciences, Bratislava, Slovakia

ARTICLE INFO

Article history:
Received 13 May 2011
Received in revised form 14 June 2011
Accepted 16 June 2011
Available online 22 June 2011

Keywords:
MgB_2
Filamentary wire
Filament density
Filament uniformity
Critical currents

ABSTRACT

Filamentary MgB_2/Ti/Glidcop wire has been manufactured by in situ process using hydrostatic extrusion, cold drawing and finally subjected to high pressure and standard densifications. Filament density of as-deformed wires was evaluated by micro-hardness measurements and related to applied deformation. It was found that filament's density and uniformity in as-deformed wire have a strong effect on the critical current density (J_c) of annealed samples. The highest J_c was measured for the filaments densified by cold isostatic pressing with 2 GPa and also for rotary swaged ones showing the best uniformity. Presented results showed the importance of filament density and homogeneity and also demonstrate suitability of hydrostatic extrusion for uniform long-length filamentary MgB_2 wires production.

1. Introduction

Low T_c filamentary superconductors, such as Nb-based, usually assembled from metallic elements are commonly deformed by extrusion followed by wire drawing [1,2]. Application of extrusion and drawing sequence for wires containing powdered filaments (e.g. PIT process) is more complicated due to high density of as-extruded filaments, which can crack or break during the consequent drawing as it was observed for BSCCO/Ag wire [3]. Similar problem may arise when drawing previously extruded MgB_2 wire. Instead of possible cracks generation, this deformation is not able to keep the powdered filament density on the sufficiently high level needed for high transport currents [4]. There are two commercial companies Hyper Tech [5] and Columbus Superconductors [6] producing MgB_2 wires in km lengths. Hyper Tech company uses a patented process for manufacturing MgB_2 and this process is called the continuous tube filling and forming (CTFF) [5] and Columbus Superconductors is using multiple rolling or drawing for ex situ based powder-in-tube process [6]. No literature data presenting the application of hydrostatic extrusion for long-length production of MgB_2 wires have been published yet. Several experiments with extruded single-core [7–9] and also 7-filament wires using ex situ and/or in situ process have been done [10,11]. These hydrostatically extruded wires with Fe and Nb/Cu sheaths had not yet sufficient filament uniformity after drawing and/or rolling [11]. It was shown that filament density prior to the final heat treatment can increase the final current densities in MgB_2 [12,13]. While the cold high pressure densification (CHPD) by 1.85 GPa was able to increase the critical current density, J_c, of MgB_2/Fe wire by more than factor of 2 at 4.2 K [12], only around 10% J_c improvement has been obtained for MgB_2/Ti tape subjected to cold isostatic pressing (CIP) by 1.5 GPa [13]. Improved transport properties have been shown also for high filament density stainless steel (SS) sheathed and cold drawn MgB_2 wires subjected to several deformations without tension stress [14].

This contribution presents the property of 30-filament MgB_2/Ti/Glidcop wire made by hydrostatic extrusion followed by cold drawing and finally densified by high pressure treatments and by standard deformations.

2. Experimental

Composite billet containing 30-filaments was assembled from single-core Ti sheathed in situ wires containing a mixture of Alfa Aesar 99% pure Mg and B powders (in stoichiometric ratio) and 8 wt% of SiC (≈20 nm) addition. Single-core wires were inserted into the Glidcop tube of 15/11 mm outer/inner diameter, see Fig. 1(a). Glidcop is copper reinforced by Al_2O_3 powder and its strength and conductivity are influenced contrary (increasing strength and decreasing conductivity) by the alumina content. Glidcop AL-60 containing 1.1 wt% of Al_2O_3 was used in this experiment [15]. Assembled billet was initially isostatically pressed (CIP) by 1.5 GPa/1.5 min, which has reduced the composite diameter from 15 to 14 mm. CIPed billet was then hydrostatically extruded (HE) into the wire of 6.9 mm, see the cross-section shown by Fig. 1(b). HE wire (containing 63.3% of Glidcop, 24.3% Ti-barrier and 12.4% of Mg–B–SiC filaments) was then cold drawn up to the diameter of 1.38 mm (D) with

* Corresponding author.
E-mail address: Pavol.Kovac@savba.sk (P. Kováč).

0925-8388/$ – see front matter © 2011 Elsevier B.V. All rights reserved.
doi:10.1016/j.jallcom.2011.06.071

several intermediate annealing (IA) at 480 °C/45 min. As-drawn wire of 1.38 mm diameter (shown by Fig. 1(c)) was finally subjected to several filament's densifications by: isostatic pressing (CIP), extrusion (HE), groove rolling (GR), two-axial rolling (TAR) and rotary swaging (RS). Main parameters applied for high pressure treated (HPT) and standardly deformed (SD) wires are given in Tables 1A and 1B, respectively. AR in Tables 1A and 1B means the resulting area reduction by applied deformation in %.

Optical microscopy and Vickers microhardness measurements HV 0.05 (5 g, 20 s) were used for the cross-section studies of deformed wires. HV 0.05 of filaments, Ti-barrier and Glidcop sheath are summarized by Table 2. Averaged HV 0.05 values were measured separately for the outer and inner filaments (see Fig. 1) and their ratio (out/in) is compared in the last column of Table 2.

X-ray micro-tomography measurement device Nanotom 180 equipped with nano-focusing X-ray tube and maximal accelerating voltage 180 kV [16] was used for non destructive analysis of several wires [17]. Wires under test were stepwise turned around the rotation axis at a small selected angle (e.g. 15′ and rotated totally at 360°) and so called X-ray projections were measured. After obtaining all necessary projections the volume image was constructed based on the inverse Radon transformation and resulting 3D image allows observing well the composite uniformity.

Short wire samples (≈70 mm) were finally heat treated (HT) at 800 °C/0.5 h in pure Ar atmosphere and transport critical currents were measured at liquid He temperature and external field between 3.5 T and 8.0 T using 1 μV cm^{-1} criterion.

3. Results and discussion

3.1. Filaments density and uniformity

Averaged HV 0.05 values of composite elements obtained from several measurements are summarized in Table 2. The HV 0.05 data demonstrate how the Glidcop sheath, Ti-barrier and density of Mg–B filaments are influenced by the applied deformation. While the hardness of Glidcop sheath is changing only slightly (190–204), Ti-barrier is more affected by work hardening and also by intermediate annealing (128–233). It is evident that filament hardness sensitively reflects the applied deformation (60–184) due to changed powder density. The lowest filament density was found

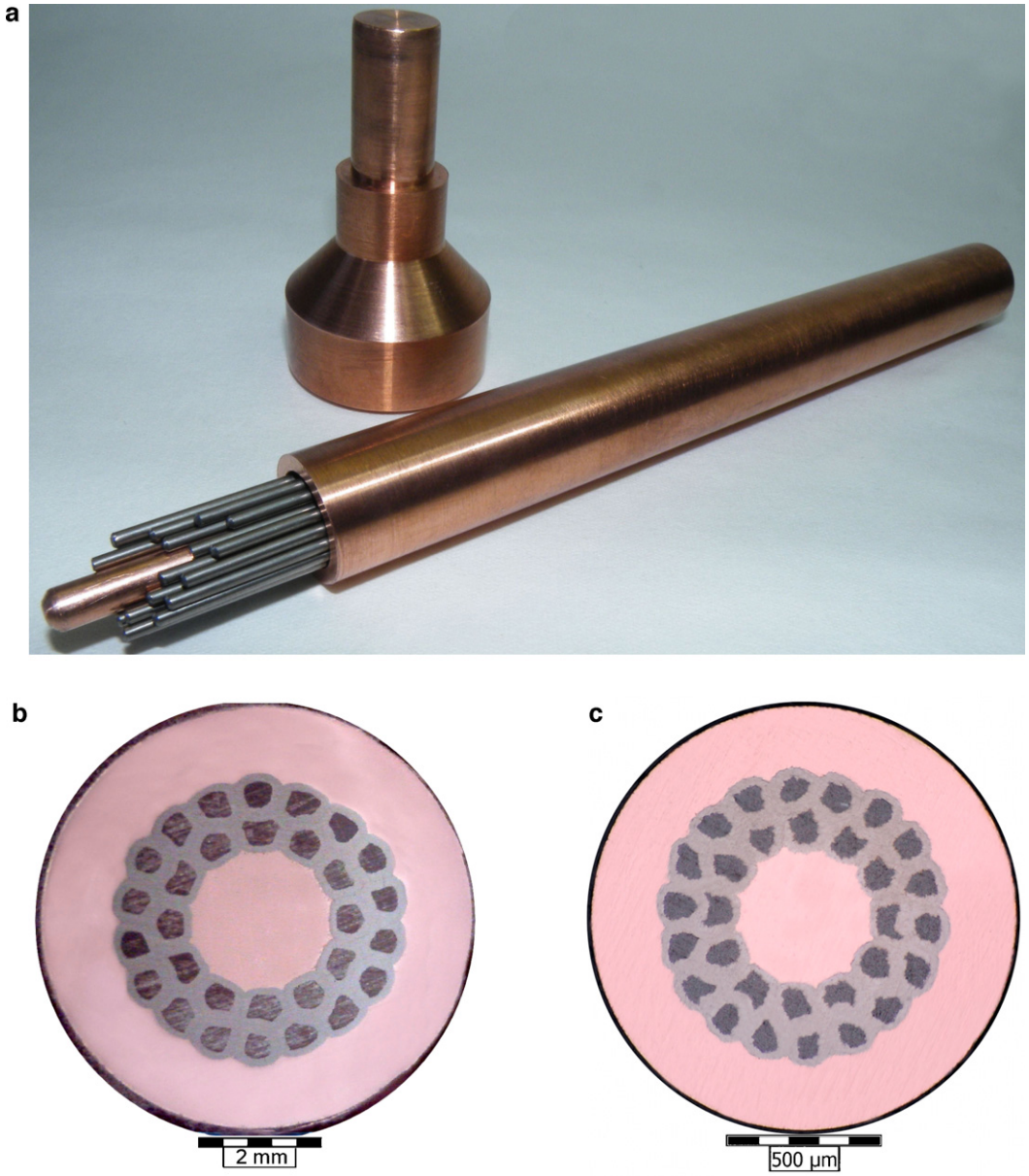

Fig. 1. Composite billet assembly containing 30 Mg–B/Ti wires placed around the central Glidcop rod and immersed in Glidcop tube (a), cross-section of hydrostatic extruded 30-filament wire of 6.9 mm (b) and cross-section of cold drawn wire 1.38 mm (c).

Table 1A
Main parameters of all applied high pressure treatments (HPT).

HPT	CIP1	HE1	CIP2	HE2	HE3	HE4
p [MPa]	1500	1330	2000	523	998	970
d_1 [mm]	15	14	1.38	1.38	1.205	1.38
d_2 [mm]	14	6.9	1.365	1.205	1.02	1.02
AR [%]	12.88	75.71	2.16	23.75	28.35	45.37

AR – area reduction, d_1 – initial diameter and d_2 – final diameter.

Table 1B
Description of MgB_2 wires subjected to standard deformations (SD).

SD	GR1	TAR1	RS1	RS2	RS3
d_1 [mm]	1.38	1.1 × 1.1	1.38	1.33	1.38
d_2 (a_2) [mm]	1.1 × 1.1	0.77 × 0.77	1.33	1.13	1.13
AR [%]	19.0	51	7.1	27.8	32.9

AR – area reduction, d_1 – initial diameter and d_2 – final diameter or final size (d_2).

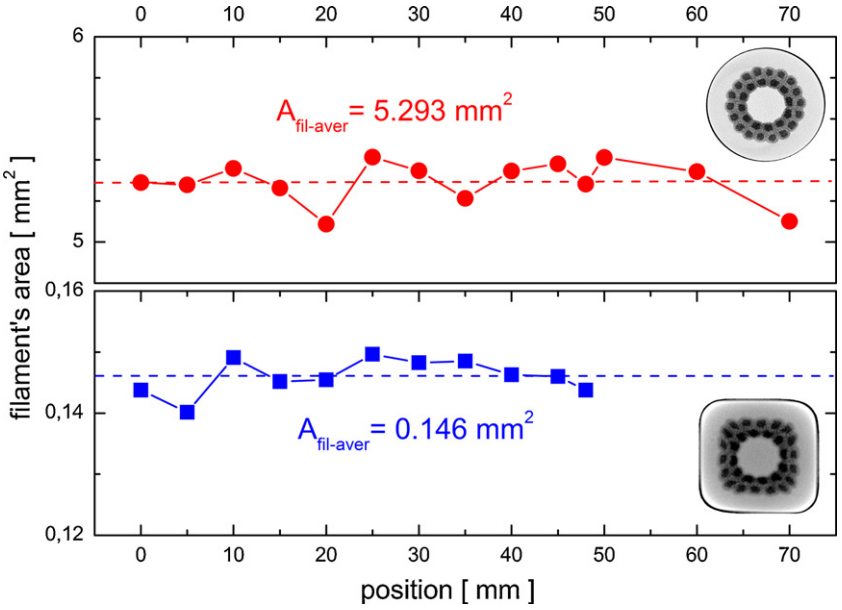

Fig. 2. Filament's area obtained by X-ray micro-tomography along the wire axis after hydrostatic extrusion (HE1, 6.9 mm) and groove rolling (GR2, 0.77 mm × 0.77 mm and heat treatment), the inserts show the transversal sections of both wires obtained by X-ray.

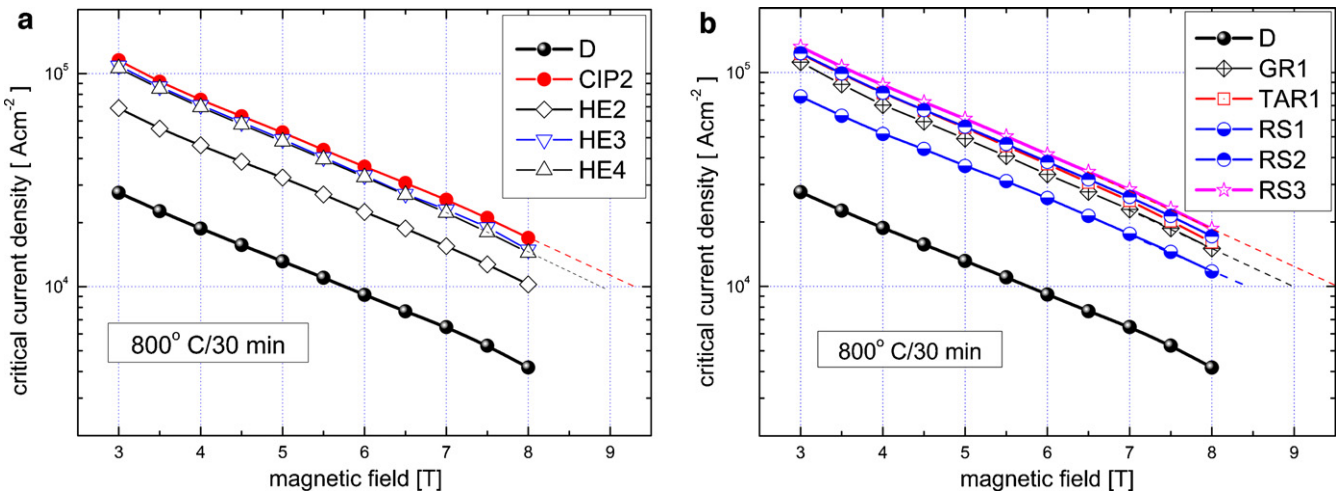

Fig. 3. Critical current densities of wires subjected to high pressure treatments (a) and to several common deformations (b) compared to drawn wire D.

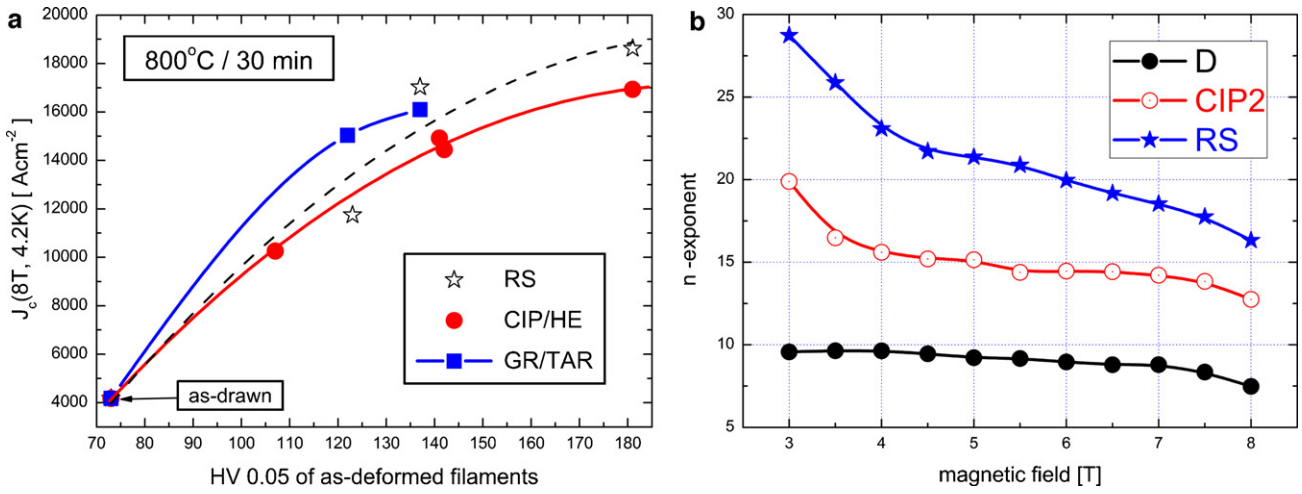

Fig. 4. Comparison of J_c (8 T) versus the filament's microhardness affected by CIP, HE, GR and RS (a) and n-exponents derived from I–V curves of drawn (D), cold pressed (CIP2) and rotary swaged (RS2) wire.

in as-drawn (D) wires (60–83, increased to 80–109 by IA) and the highest ones for the wires subjected to CIP2 (178–185) and RS3 (168–194). Although low temperature was used for IA (480 °C), the filament hardness is increased due to partial reaction between Mg and B, see Table 2. Comparison of HV 0.05 between inner and outer filament rings gives useful information about the filament's homogeneity. The worse homogeneity is observed for as-drawn wires (out/in: 1.28–1.38, see Table 2), which can be attributed to small applied area drawing reductions per pass (rpp < 10%) increasing more the density in outer filaments. As one can see, all deformations applied after wire drawing has increased effectively the filament's density and improved the homogeneity as well. Surprisingly, the best filament uniformity was observed for wires deformed by rotary swaging RS1 and RS2 (out/in: 0.993–1.00). The total area reduction by rotary swaging above 30% makes the filaments denser but less uniform (see out/in: 1.154 for RS3). In comparison to other used deformations, RS is characterized by vibrating and rotating hammer hits, which densify the filaments "dynamically" and consequently more effectively and uniformly. Dense and uniform filaments were obtained also by two-axial rolling of wire GR1 from 1.1 mm down to 0.77 mm with AR = 51% (see the last row in Table 2, out/in: 0.993).

The resulting 3D images obtained from X-ray microtomography were used for observing the filament's uniformity along the wire length. Short videos made from the images data of tested wires allowing to see any change in the wire cross-section and especially the filament's area variation. Filament area at some positions of 3D image was estimated more precisely by software analysis and is plotted by Fig. 2 along the wire axis of two samples HE1 and GR1 heat treated at 800 °C/0.5 h. Fig. 2 presents an excellent filament's uniformity of both wires, which is only ±3% of averaged filament area and confirms the suitability of hydrostatic extrusion for long lengths and uniform filamentary MgB_2 wires production by PIT technique.

3.2. Critical current densities

Transport critical current (I_c) measurements of ≈70 mm long wire samples were done by using 1 μV cm^{-1} criterion. Critical current densities (J_c) at variable external field were evaluated by dividing the I_c value with the whole filaments area. Fig. 3(a) and (b) presents $J_c(B)$ characteristics of drawn (D), additionally high pressure treated (CIP and HE) and commonly deformed (GR, TAR and RS) wires, respectively. It is evident that $J_c(B)$ of D wire ($J_c = 10^4$ A cm^{-2} at 5.75 T) is considerably increased by applied extrusions HE2–HE4 and most effectively by CIP2 giving $J_c = 10^4$ A cm^{-2} at 9.3 T, see Fig. 3(a). While the area reduction AR = 23.75% by extrusion at 523 MPa applied for wire HE2 shifts J_c of 10^4 A cm^{-2} from 5.75 to 8 T, increased pressure to ≈1 GPa and AR = 28.35–45.77% used for HE3 and HE4 are able to reach 10^4 A cm^{-2} at 9 T. Similar scale of AR by groove rolling, two-axial rolling and by rotary swaging was applied for D wire 1.38 mm described in Table 1B. Comparable J_c improve-

Table 2
HV 0.05 values of composite elements measured after variable deformations (CIP, HE, D, GR, TAR and RS), IA – intermediate annealing applied at 480 °C/45 min, out/in – the ratio of HV 0.05 measured in outer and inner filaments ring.

Wire size [mm]	Deformed/annealed	HV 0.05				
		Glidcop	Ti	Filam-out	Filam-in	Out/in
6.9	HE1	190	233	132	141	0.936
6.9	HE1 + IA	176	233	182	157	1.159
2.25	HE1 + D	195	186	83	60	1.383
2.25	HE1 + D + IA	196	196	109	80	1.362
1.38	HE1 + D + IA	204	128	82	64	1.281
1.365	HE1 + D + CIP2	199	130	185	178	1.039
1.33	HE1 + D + RS1	202	204	123	123	1.000
1.205	HE1 + D + HE2	196	186	113	101	1.089
1.13	HE1 + D + RS2	204	214	137	138	0.993
1.13	HE1 + D + RS3	205	220	194	168	1.154
1.02	HE1 + D + HE2 + HE3	196	205	154	128	1.080
1.02	HE1 + D + HE4	202	208	148	137	1.080
1.1 × 1.1	HE1 + D + GR1	190	181	130	115	1.130
0.77 × 0.77	HE1 + D + GR1 + TAR1	200	234	137	138	0.993

ments as for high pressure treatments were reached by standard deformations GR, TAR and especially by RS, see Fig. 3(b). Quite small AR ≈ 7% by RS1 gives higher J_c improvement than HE2 with AR = 23.75% (see Table 1A). GR with AR = 19% shifts J_c of 10^4 A cm^{-2} to 9.0 T as for HE3 and HE4 with pressure ≈1 GPa. The highest J_c was measured for RS3 wire with total AR ≈ 33% reaching 10^4 A cm^{-2} at ≈9.5 T. Presented results clearly show that Mg–B filaments densification by high pressure treatments is not able to increase the transport currents more effectively than by standard rolling or rotary swaging.

Fig. 4(a) compares J_c (8 T) versus the filament's hardness of differently deformed wires. First of all, it shows a direct positive effect of the filament hardness (density) on the final transport current densities. Less pronounced effect of filaments densification was presented for stainless steel (SS) sheathed multi-core MgB_2 wires [14]. J_c (8 T) of drawn high filament density SS sheathed wire was increased maximally by 10–17% using high pressure densification [14]. Generally, the effect of filament densification is less effective if as-drawn filaments are already dense (HV 0.05 = 188 for SS sheathed wire) in comparison to low density filaments (e.g. HV 0.05=70 for Glidcop sheathed one). In the case of presented 30 filament wire with Glidcop sheath, the maximal improvements of J_c (8 T) are much larger: 387% by TAR1, 407% by CIP2 and 447% by RS3 mode. RS wires show simple and most effective way for J_c improvement in low density (as-drawn) wires. It can be explained by two positive effects of rotary swaging: increased filament density and improved uniformity, which results in the best grain-connectivity controlling the transport current density. Fig. 4(b) shows the comparison of *n*-exponents derived from *I*–*V* curves measured for D, CIP2 and RS2 wires. The *n*-exponent characterizes the sharpness of the *I*–*V* curve, where the voltage rise is not only due to flux motion in the superconductor but also influenced by current sharing inside or among the non-uniform filaments. It means, that *n*-exponent can reflect sensitively the filament uniformity. In our case, *n*-exponent of CIP2 wire is by 50% higher than for D wire and is more than doubled in RS2, which confirms the better uniformity of MgB_2 filaments. It should be mentioned that not only filament's density (influenced by the applied pressure) is decisive for final J_c values. There are also secondary phases, e.g. MgB_4 and MgO reducing the current path and consequently decreasing J_c [18].

4. Conclusions

Uniform multi-core MgB_2/Ti/Glidcop wires have been produced by in situ approach process using hydrostatic extrusion followed by high pressure and conventional densifications. It is demonstrated that low filament density in as drawn wire could be increased effectively by isostatic pressing, extrusion, rolling and rotary swaging. It was found that the final filament's density and uniformity influences the grain connectivity and consequently critical current density is increased remarkably (more than 4 times). The highest J_c's were measured for the wire isostatically pressed by 2 GPa and also for the rotary swaged wire in which the filament's homogeneity is the best. Presented results clearly demonstrate suitability of hydrostatic extrusion for future production of long-lengths and uniform filamentary MgB_2 wires applicable for coils.

Acknowledgement

This work was supported by the Slovak Scientific Agency under projects APVV-0495-10 and APVV-0647-10 and by project FU07-CT-2007-0031.

References

[1] M. Suenaga, A.F. Clark, Filamentary A15 Superconductors, Plenum Press, New York, 1980.
[2] J.A. Parrell, et al., IEEE Trans. Appl. Supercond. 19 (2009) 2573.
[3] I. Hušek, P. Kováč, W. Pachla, Supercond. Sci. Technol. 8 (1995) 617.
[4] I. Hušek, P. Kováč, C.R.M. Grovenor, L. Goodrich, Supercond. Sci. Technol. 17 (2004) 971.
[5] http://www.hypertechresearch.com/page4.html.
[6] http://www.columbussuperconductors.com/mgb2.htm.
[7] W. Pachla, P. Kováč, R. Diduszko, A. Mazur, I. Hušek, A. Morawski, A. Presz, Supercond. Sci. Technol. 16 (2003) 7.
[8] W. Pachla, P. Kováč, A. Mazur, I. Hušek, T. Melišek, V. Štrbík, M. Müller, A. Presz, Supercond. Sci. Technol. 18 (2005) 552.
[9] W. Pachla, A. Morawski, P. Kováč, I. Hušek, A. Mazur, T. Lada, R. Diduszko, T. Melišek, V. Štrbík, M. Kulczyk, Supercond. Sci. Technol. 19 (2006) 1.
[10] P. Kováč, I. Hušek, W. Pachla, M. Kulczyk, Supercond. Sci. Technol. 20 (2007) 607.
[11] P. Kováč, W. Pachla, I. Hušek, T. Melišek, M. Kulczyk, T. Holubek, R. Diduszko, M. Reissner, Physica C 468 (2008) 2356.
[12] R. Flükiger, M.S.A. Hossain, C. Senatore, Supercond. Sci. Technol. 22 (2009) 085002.
[13] J. Viljamaa, P. Kováč, I. Hušek, T. Melišek, V. Štrbík, J. Phys: Conf. Ser. 234 (2010) 022041.
[14] P. Kováč, I. Hušek, T. Melišek, L. Kopera, M. Reissner, Supercond. Sci. Technol. 23 (2010) 065010.
[15] http://www.hoganas.com/en/Products–Applications/GLIDCOP/.
[16] http://www.ge-mcs.com/en/radiography-x-ray/ct-computed-tomography/nanotom-s.html.
[17] M. Hain, M. Nosko, F. Simančík, T. Dvorák, R. Florek, Proceedings of the Conference Measurement 2011, Smolenice, 27–30 April, 2011.
[18] M. Eisterer, Supercond. Sci. Technol. 20 (2007) R47–R73.